Fatigue Mechanism of Antiferroelectric $Hf_{0.1}Zr_{0.9}O_2$ Toward Endurance Immunity by Opposite Polarity Cycling Recovery (OPCR) for eDRAM

K.-Y. Hsiang, *Graduate Student Member, IEEE*, J.-Y. Lee, Z.-F. Lou, F.-S. Chang, Y.-C. Chen, Z.-X. Li, M. H. Liao, *Member, IEEE*, C. W. Liu, *Fellow, IEEE*, T.-H. Hou, *Senior Member, IEEE*, P. Su, *Member, IEEE*, and M. H. Lee, *Senior Member, IEEE*

***Abstract*— Opposite polarity cycling recovery (OPCR) is proposed to completely restore a fatigued antiferroelectric (AFE) capacitor back to its initial state, thereby extending the endurance number of switching cycles for AFE-RAM. A comprehensive model exclusive to AFE with unipolar cycling is revealed to achieve unlimited endurance, and the unipolar cycling with OPCR is experimentally demonstrated to accumulate 10^{12} cycles, while achieving the nondegradation and complete restoration of the remnant polarization (P_r). Furthermore, the proposed OPCR achieves a recovery time ratio of 0% ($t_{recovery}/t_{period}$), which indicates no extra time to spend for the recovery procedure.**

***Index Terms*— Antiferroelectric (AFE), endurance, recovery.**

I. Introduction

RECENTLY, ferroelectric (FE) materials have been extensively investigated as candidates for future-generation emerging memory applications. The wake-up effect and cycling fatigue inevitably result in lead performance degradation, and these mechanisms involve domain pinning and a stress-induced leakage current (SILC), which are dominated by oxygen vacancy (VO) disturbances [1], [2]. Recently, several techniques have been reported that redistribute VO for the recovery of FE characteristics to extend the switching cycle number in FeRAM [3], [4], [5]. The wake-up and fatigue mechanism model for most publications is illustrated in Fig. 1(a) [3], [4], in which the magnitude of the VO location plays an important role in low electric field (E-field) cycling. Subsequently, the redistribution of VO can be performed by high E-field stimulation to achieve recovery from domain pinning [3], [4]. For antiferroelectric (AFE) materials, a faster dipole switching speed and robust endurance have been reported compared with FE materials [6], [7]. The AFE fatigue is experimentally measured and follows the model with bipolar cycling and low E-field operation as shown in Fig. 1(b). However, the insufficient AFE recovery procedure creates an enormous gap from the initial state by high E-field stimulation, as shown in Fig. 1(c). Therefore, the scheme procedure for AFE must be optimized to restore polarization more effectively for maximum cycling endurance. In this work, an opposite polarity cycling recovery (OPCR) is proposed, and the fatigue mechanism for long/high endurance applications is investigated.

Manuscript received 16 November 2022; revised 4 January 2023; accepted 16 January 2023. Date of publication 30 January 2023; date of current version 24 March 2023. This work was supported in part by the National Science and Technology Council (NSTC) under Grant 111-2218-E-A49-016-MBK, Grant 111-2221-E-003-031-MY3, and Grant 111-2622-8-002-001; and in part by Taiwan Semiconductor Research Institute (TSRI) and Nano Facility Center (NFC), Taiwan. This article is an extended version of a paper presented at IEDM 2022. The review of this article was arranged by Editor G. Meneghesso. *(Corresponding author: M. H. Lee.)*

K.-Y. Hsiang is with the Institute of Electronics, National Yang Ming Chiao Tung University, Hsinchu 300, Taiwan, and also with the Graduate School of Advance Technology, National Taiwan University, Taipei 10617, Taiwan.

J.-Y. Lee and C. W. Liu are with the Graduate School of Advance Technology, National Taiwan University, Taipei 10617, Taiwan.

Z.-F. Lou, F.-S. Chang, Z.-X. Li, and M. H. Lee are with the Institute of Electro-Optical Engineering, National Taiwan Normal University, Taipei 11677, Taiwan (e-mail: mhlee@ntnu.edu.tw).

Y.-C. Chen, T.-H. Hou, and P. Su are with the Institute of Electronics, National Yang Ming Chiao Tung University, Hsinchu 300, Taiwan.

M. H. Liao is with the Department of Mechanical Engineering, National Taiwan University, Taipei 10617, Taiwan.

Color versions of one or more figures in this article are available at https://doi.org/10.1109/TED.2023.3238364.

Digital Object Identifier 10.1109/TED.2023.3238364

II. Experimental Procedure

A metal–(anti)ferroelectric–metal (M(A)FM) capacitor was employed. A 2-nm TiN layer was initially deposited by atomic layer deposition (ALD) as the bottom electrode (BE). Then, 10-nm $Hf_{1-x}Zr_xO_2$ (HZO) films were deposited on the BE by ALD at 250 °C, where the HfO_2:ZrO_2 ratio was 1:1 and 1:9 for the FE and AFE layers, respectively. Subsequently, an 80-nm TiN top electrode (TE) was covered on the prior HZO layer by a sputtering system. Finally, annealing was performed at 550 °C in ambient Ar for 60 s by rapid thermal annealing (RTA) for HZO crystallization.

Fig. 2(a) and (b) shows the P–V characteristics of HZO with Zr = 50% and 90% for bipolar and unipolar sweeps,

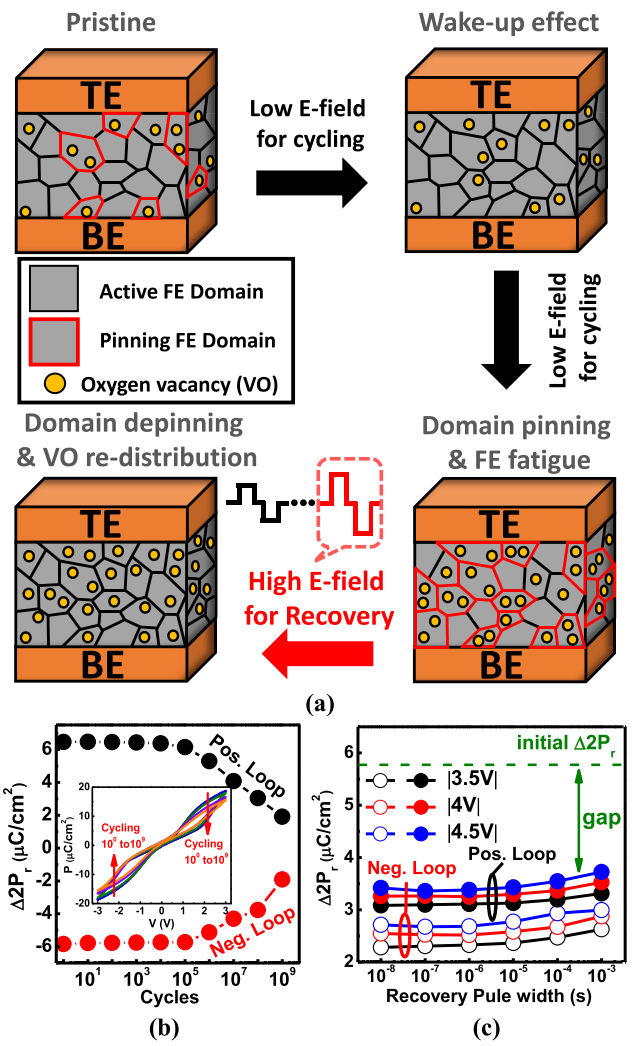

Fig. 1. (a) Wake-up and fatigue mechanism model in most publications [3], [4]. The magnitude and location of VOs play an important role. The redistribution of VO can be performed by a high *E*-field stimulation to achieve recovery from domain pinning away [3], [4]. (b) Endurance characteristics of AFE with bipolar cycling and low *E*-field operation. (c) Insufficient AFE recovery procedure creates an enormous gap from the initial state by high *E*-field stimulation.

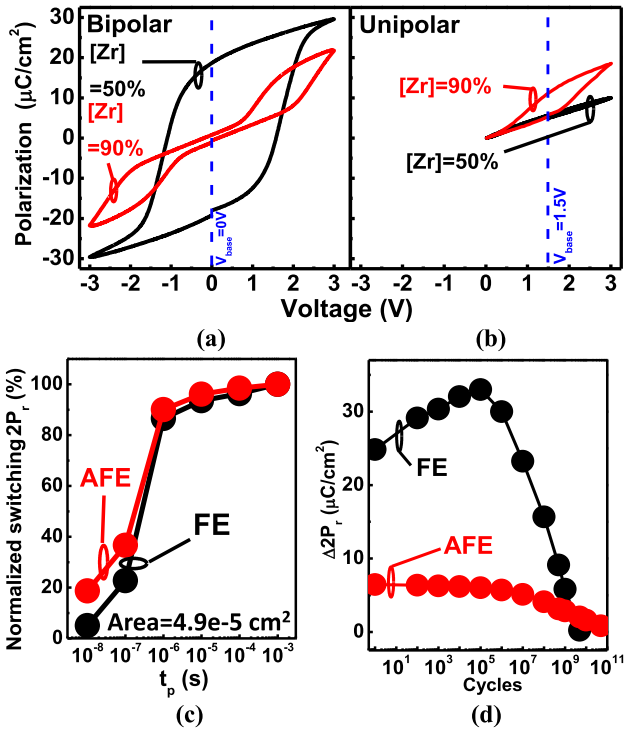

Fig. 2. P–V of Zr = 50% and 90% of HZO for (a) bipolar and (b) unipolar sweeps. For the unipolar sweeps, Zr = 50% and 90% show a nearly paraelectric and single loop, respectively [8]. (c) Available ratio of AFE switching polarization is obviously higher than FE with $t_p < 1$ μs [6], [7]. (d) Higher AFE cycling number is measured and compared with FE cycling to validate the robust AFE endurance.

respectively. For bipolar operation, the typical FE and AFE characteristics are exhibited with bipolar sweeps for Zr = 50% and 90%, respectively. For the unipolar sweeps, Zr = 50% and 90% show a nearly paraelectric and single loop, respectively [8]. Therefore, Zr = 50% and 90% HZO are denoted as FE and AFE in this work, respectively. The FE and AFE speed responses are shown in Fig. 2(c), where is the normalized $2P_r$ versus programming pulse width (t_p). The available ratio of AFE switching polarization is obviously higher than that of FE with $t_p < 1$ μs [6], [7]. To maintain high FE and AFE switching ratios, the pulse condition was selected as $t_p = 1$ μs with 1/4 MHz for subsequent recovery testing. Since VOs are located near the interface of TiN and HZO to stabilize the AFE tetragonal phase, the higher AFE cycling number is measured and compared with the FE to validate the robust AFE endurance, as shown in Fig. 2(d) [7], [9].

III. Results and Discussion

A. Independence Polarity of Positive and Negative Loops in AFE Systems

Fig. 3(a)–(d) shows the PUND P–V characteristics and $2P_r$ versus switching cycles of the AFE, respectively. Note that the base voltages (V_{base}) of positive and negative unipolar cycling are 1.5 and −1.5 V, respectively, and the corresponding pulse sequences are shown in the insets of Fig. 3(a) and (b). Significant degradation for ⓒ after cycling of the same polarity is observed; however, ⓓ maintains the initial state with the opposite polarity. In addition, the SILC also increases after cycling of the same polarity, but the leakage current density (J) with opposite polarity remains almost unchanged, as shown in Fig. 3(c) and (d). In summary, the positive and negative AFE loops exhibit independent polarities on fatigue and SILC by domain switching degradation and leakage paths with VO accumulation. This indicates that the individual domains are responsible for positive and negative polarity in the AFE system, and the VO-induced SILC increases for the same polarity.

B. Opposite Polarity Pulse Recovery (OPPR) for AFE

Due to insufficient recovery by high E-field stimulation in Fig. 1(c), OPPR is proposed for comparison and illustrated in Fig. 4(a). The increase in pulse amplitude and width (time) indeed benefits recovery and approaches the initial state of $2P_r$ and J [10]. However, there is still a nonneglected gap for

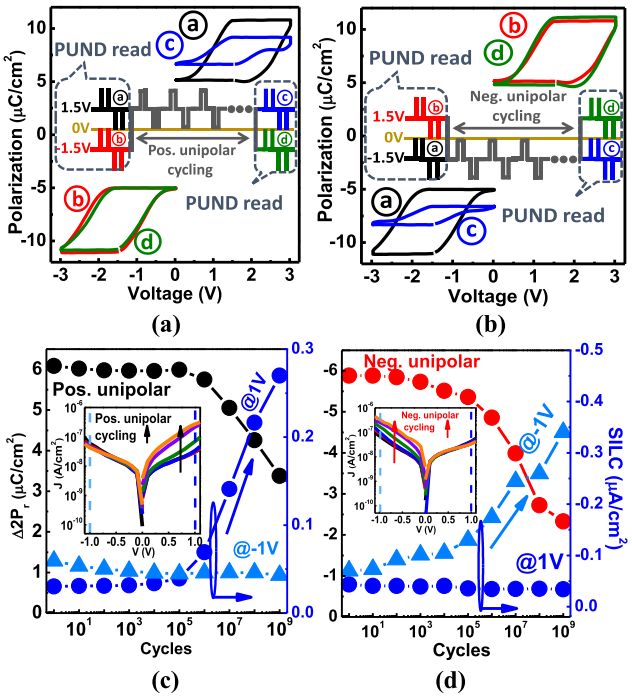

Fig. 3. (a) and (b) PUND P–V characteristics and (c) and (d) $2P_r$ versus switching cycles of the AFE. The base voltages (V_{base}) of positive and negative unipolar cycling are 1.5 and −1.5 V, respectively. (a) and (b) Significant degradation for ⓒ after cycling of the same polarity cycling is observed; however, ⓓ maintains the initial state with opposite polarity. (c) and (d) SILC also increases after cycling of the same polarity, but the leakage current density (J) with opposite polarity remains almost unchanged.

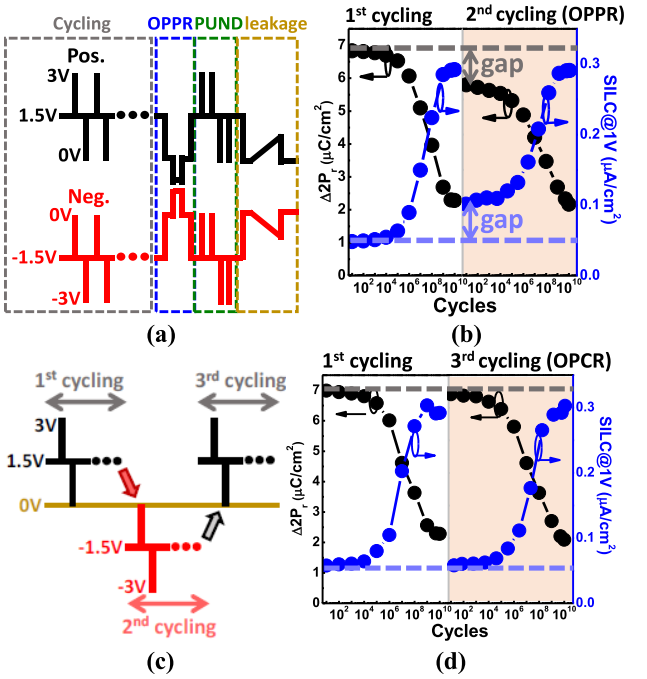

Fig. 4. (a) OPPR is proposed for comparison. (b) OPPR-based recovery for twice 1×10^{10} cycles of positive unipolar cycling. OPPR has improved the recovery compared to high E-field stimulation, as shown in Fig. 1(c); however, the incomplete return back to the initial states of $2P_r$ and SILC is still an issue. (c) Pulse sequence of OPCR. (d) OPCR-based recovery for the first and third periods with 1×10^{10} cycles of twice positive unipolar cycling.

both $2P_r$ and J. Based on OPPR, positive unipolar cycling with 1×10^{10} cycles for endurance was performed for two periods, as shown in Fig. 4(b), which shows a gap between the first and second periods. This implies that the degradation would lead to a finite number for endurance. OPPR improved the recovery compared to high E-field stimulation, as shown in Fig. 1(c); however, the incomplete return to the initial states of $2P_r$ and SILC is still an issue.

C. OPCR for AFE

Sufficient recovery is in high demand for the high endurance of eDRAM applications. OPCR is proposed to pursue complete restoration to the initial state, which operates on a fatigued device under test (DUT) by alternate polarity cycling, as shown in Fig. 4(c). Fig. 4(d) shows the results of recovery via OPCR for the first and third periods with 1×10^{10} cycles of two positive unipolar cycling periods. The same magnitude of $2P_r$ and SILC are measured after OPCR to validate sufficient recovery.

D. Fatigue Mechanism of AFE $HfZrO_2$

According to previous research reports, the FE fatigue and degradation are dominated by (i) the m-phase increment, (ii) breakdown, and/or (iii) dipole pinning, as shown in Fig. 5(a) [1], [3], [4], [11], [12], [13], [14], [15], [16]. Three fatigue mechanisms are discussed for AFE and validated by experimental measurements as follows.

For (i) m-phase formation, the lattice dislocation is located in the FE orthorhombic phase (o-phase) grain with a large grain size to form the non-FE monoclinic phase (m-phase) with cycling to lead to endurance fatigue for FE $Hf_{0.5}Zr_{0.5}O_2$ [11], [12]. However, the relative permittivity remains almost unchanged with endurance cycles for the AFE, even when $2P_r$ decreases as shown in Fig. 6(a) and (b), which indicates an ignorable increment for the m-phase. For (ii) breakdown, the dipole switching becomes invalid within a domain due to filament-base breakdown [3], [14]. Fig. 3(c) and (d) shows the SILC occurrence with cycling, but the magnitude of currents is much smaller than the hard breakdown in Fig. 6(c). Note that the condition of hard breakdown is 10 MV/cm. Furthermore, filament path formation requires an abundant number of VOs in the AFE capacitor. For (iii) dipole pinning, the increment of VOs and injected charges may lead to domain pinning with P_r degradation [1], [3], [4], [14], [15], [16]. The VO is confirmed to be unchanged before and after cycling, as shown in Fig. 6(d), which is extracted by oxygen 1 s X-ray photoelectron spectroscopy (XPS) spectra. This indicates no additional VO generation during cycling; therefore, the redistribution of VO in the domain dominates the mechanism.

Fig. 5(b) shows a comprehensive model for high E-field stimulation, OPPR, and OPCR for AFE. In Fig. 3, the AFE domains can be divided into positive and negative polarities independent of the tetragonal phase, which is notably different from the orthorhombic-based FE system. For the recovery by high E-field stimulation on bipolar AFE cycling, VOs are

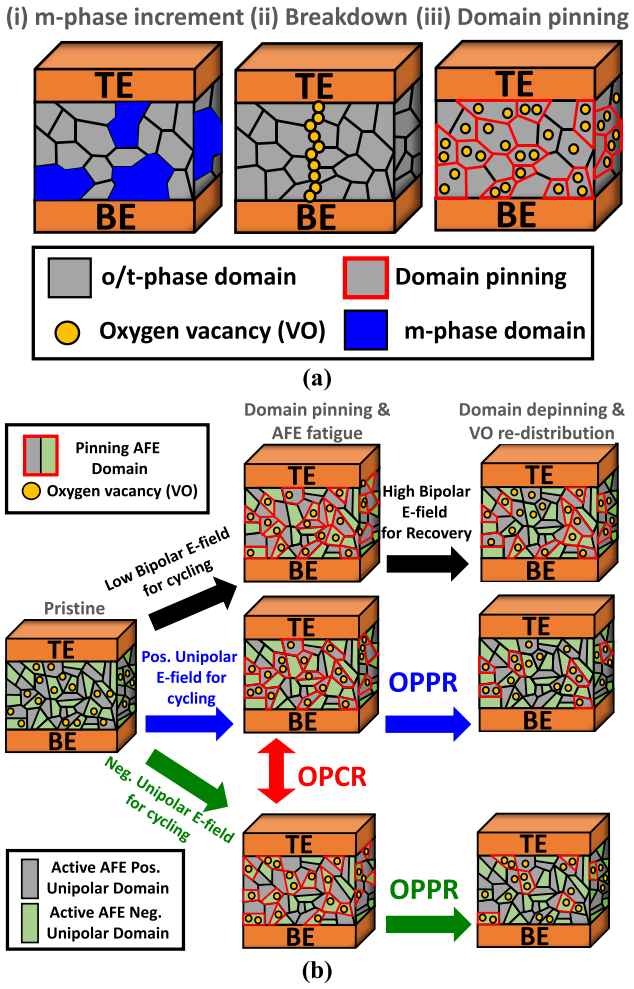

Fig. 5. (a) According to previous research reports, the FE fatigue and degradation are dominated by (i) *m*-phase increment, (ii) breakdown, and/or (iii) dipole pinning [1], [3], [4], [11], [12], [13], [14], [15], [16]. (b) Comprehensive model for AFE fatigue and recovery with high *E*-field stimulation (black path), OPPR (blue and green paths), and OPCR (red path). The AFE domains can be divided into positive and negative polarities independently with *t*-phase according to Fig. 3.

randomly redistributed in the positive and negative polarity domains as shown in the black path of Fig. 5(b). However, most of the domains are still pinned, indicating insufficient recovery, as shown in Fig. 1(c). The blue and green paths of Fig. 5(b) show the OPPR with unipolar cycling operation for positive and negative polarities, respectively. Due to the unipolar cycling operation, VO accumulates in corresponding domains and leads to leakage path formation. The nonoperated domain of opposite polarity remains almost unchanged, as shown in Fig. 3(c) and (d). Although most of the VOs have been redistributed for domains depinning after OPPR, $2P_r$ and J still exhibit incomplete returns to the initial state with a nonneglected gap, as shown in Fig. 4(b). For OPCR, the VO redistribution with opposite polarity cycling is shown as the red path in Fig. 5(b) since the total amount of VO remains unchanged with cycling. The complete VO diffusion from the occupied domain to the vacant domain with opposite polarity cycling leads to sufficient recovery while restoring the initial $2P_r$ and J, as shown in Fig. 4(d).

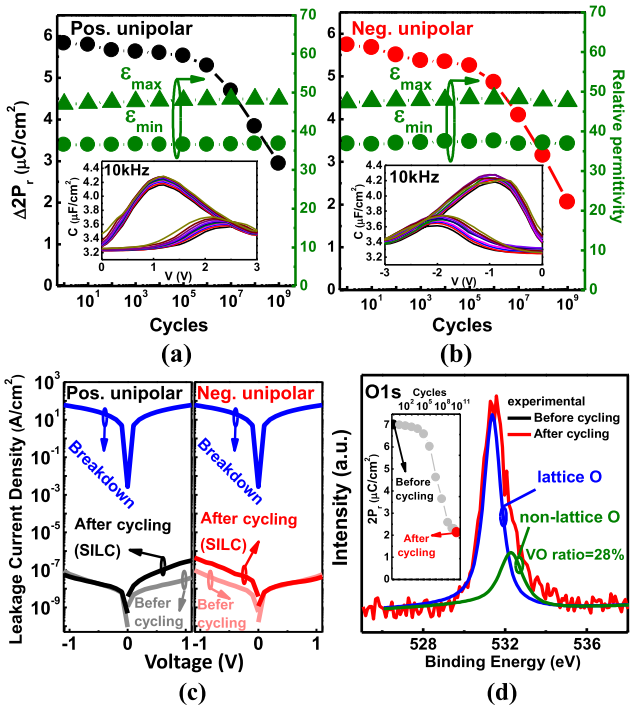

Fig. 6. Relative permittivity of (a) positive and (b) negative unipolar remains almost constant with AFE endurance cycles, even at $2P_r$ decreasing, indicating ignorable *m*-phase transition. (c) SILC occurs with cycling, but the magnitude of currents is much smaller than with a hard breakdown. (d) VOs are confirmed unchanged before and after cycling by oxygen 1 s of XPS.

TABLE I
COMPARED WITH RECOVERY TECHNOLOGIES OF PRIOR WORKS ON FE CAPACITORS, AFE UNIPOLAR CYCLING WITH OPCR NOT ONLY REDUCES THE VOLTAGE, BUT ALSO ACHIEVES A RECOVERY TIME RATIO OF 0%, WHICH INDICATES NO EXTRA TIME FOR THE RECOVERY PROCEDURE

Reference	This work	Ref. [3]	Ref. [4]
Material	AFE	FE	FE
Thickness (nm)	10	8	10
Cycling ΔV/freq.(MHz)	3V/0.25	4V/1	3.5V/5
Recovery Method (ΔV/freq. (MHz))	OPCR (3V/0.25)	High E-field (8V/1)	High E-field (7V/5)
Cycles Per Recovery (#)	2e10	1e7	1e10
Recovery time/Period (%)	0%	~0.1%	1e-6%
Cumulative cycles (#)	1e12	1e9	1e12

E. Endurance Immunity by OPCR for AFE

Fig. 7(a) shows a schematic illustration of the OPCR scheme. The alternating polarity cycling sequences for endurance and recovery with unipolar cycling for each period are shown. According to Fig. 3(c) and (d), the independent polar domains are switched and fatigued with a single period, and unaffected opposite-type domains, as well as the recovery procedure, are performed simultaneously as shown in Fig. 4(d). The purposes of each period are illustrated in the bottom half of Fig. 7(a). Therefore, the scheme of the alternating polarity of cycling for OPCR is repeated to demonstrate the performance of this model and validate the

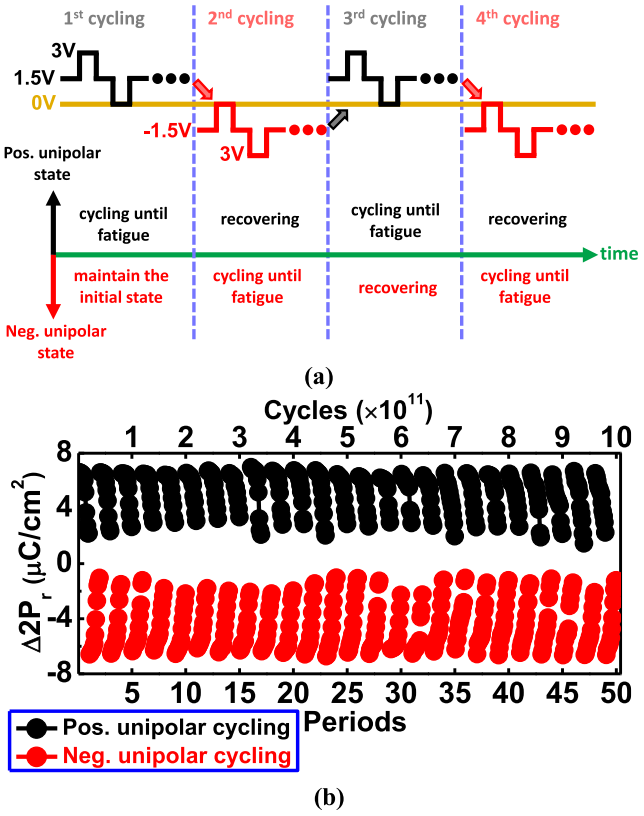

Fig. 7. (a) Schematic illustration of alternating polarity cycling sequences for OPCR. The purposes of each period are shown in the bottom half of the illustration. (b) AFE capacitor with unipolar cycling and OPCR for 50 periods with alternate polarity and accumulates to 10^{12} switching cycles.

hypothesis. Fig. 7(b) shows an AFE capacitor with unipolar cycling and OPCR for 50 periods (2×10^{10} cycles/period) with alternate polarity and accumulation to 10^{12} switching cycles. The nondegradation and complete restoration of P_r were measured to determine the prospect of unlimited endurance by OPCR.

Compared with the recovery technologies of prior works on FE capacitors, the unipolar AFE cycling with OPCR not only reduces the voltage, but also achieves a recovery time ratio of 0% ($t_{\text{recovery}}/t_{\text{period}}$), which indicates no extra time to spend for the recovery procedure as shown in Table I. Note that the frequency and pulsewidth are 1/4 MHz and 1 μs, respectively, to confirm almost complete dipole switching in Fig. 2(d), indicating a relatively rigorous stress condition compared to prior works.

IV. Conclusion

A comprehensive model is proposed for AFE cycling and recovery mechanisms including high E-field recovery, OPPR, and OPCR. The VO redistribution dominates polarization fatigue with domain pinning. The scheme OPCR provides complete restoration of the remnant polarization for AFE since the individual domains are responsible for positive and negative polarities, which is different from FE. Furthermore, the proposed OPCR with a recovery time ratio of 0% ($t_{\text{recovery}}/t_{\text{period}}$), indicating no extra time to spend for the recovery procedure. The performance of the OPCR is demonstrated for 10^{12} switching cycles with nondegradation toward unlimited endurance and validates the hypothesis. The access scheme of alternate polarity cycling for AFE-RAM is revealed for eDRAM applications.

References

[1] M. Pešić et al., "Physical mechanisms behind the field-cycling behavior of HfO_2-based ferroelectric capacitors," *Adv. Funct. Mater.*, vol. 26, no. 25, pp. 4601–4612, Jul. 2016, doi: 10.1002/adfm.201600590.

[2] M. Pesic et al., "Root cause of degradation in novel HfO_2-based ferroelectric memories," *IEEE Int. Rel. Phys. Symp. (IRPS)*, Apr. 2016, pp. MY-3-1–MY-3-5, doi: 10.1109/IRPS.2016.7574619.

[3] Y. K. Chang et al., "The field-dependence endurance model and its mutual effect in Hf-based ferroelectrics," in *Proc. IEEE Int. Rel. Phys. Symp. (IRPS)*, Mar. 2022, pp. 3A.1-1–3A.1-5, doi: 10.1109/IRPS48227.2022.9764420.

[4] P. J. Liao et al., "Characterization of fatigue and its recovery behavior in ferroelectric HfZrO," in *Proc. Symp. VLSI Technol.*, 2021, pp. 1–2.

[5] Y. Peng et al., "HfO_2-ZrO_2 superlattice ferroelectric capacitor with improved endurance performance and higher fatigue recovery capability," *IEEE Electron Device Lett.*, vol. 43, no. 2, pp. 216–219, Feb. 2022, doi: 10.1109/LED.2021.3135961.

[6] Y.-C. Chen, K.-Y. Hsiang, Y.-T. Tang, M.-H. Lee, and P. Su, "NLS based modeling and characterization of switching dynamics for antiferroelectric/ferroelectric hafnium zirconium oxides," in *IEDM Tech. Dig.*, Dec. 2021, pp. 15.4.1–15.4.4, doi: 10.1109/IEDM19574.2021.9720645.

[7] K.-Y. Hsiang et al., "Correlation between access polarization and high endurance (~10^{12} cycling) of ferroelectric and anti-ferroelectric $HfZrO_2$," in *Proc. IEEE Int. Rel. Phys. Symp. (IRPS)*, Mar. 2022, pp. P9-1–P9-4, doi: 10.1109/IRPS48227.2022.9764533.

[8] K.-Y. Hsiang et al., "Unipolar parity of ferroelectric-antiferroelectric characterized by junction current in crystalline phase $Hf_{1-x}Zr_xO_2$ diodes," *Nanomaterials*, vol. 11, no. 10, p. 2685, Oct. 2021, doi: 10.3390/nano11102685.

[9] K.-Y. Hsiang et al., "Bilayer-based antiferroelectric $HfZrO_2$ tunneling junction with high tunneling electroresistance and multilevel nonvolatile memory," *IEEE Electron Device Lett.*, vol. 42, no. 10, pp. 1464–1467, Oct. 2021, doi: 10.1109/LED.2021.3107940.

[10] K.-Y. Hsiang et al., "Novel opposite polarity cycling recovery (OPCR) of $HfZrO_2$ antiferroelectric-RAM with an access scheme toward unlimited endurance," in *IEDM Tech. Dig.*, San Francisco, CA, USA, Dec. 2022, pp. 763–766.

[11] Y. Zheng et al., "Atomic-scale characterization of defects generation during fatigue in ferroelectric $Hf_{0.5}Zr_{0.5}O_2$ films: Vacancy generation and lattice dislocation," in *IEDM Tech. Dig.*, Dec. 2021, pp. 713–761, doi: 10.1109/IEDM19574.2021.9720565.

[12] Y. Zhou et al., "The effects of oxygen vacancies on ferroelectric phase transition of HfO_2-based thin film from first-principle," *Comput. Mater. Sci.*, vol. 167, pp. 143–150, Sep. 2019, doi: 10.1016/j.commatsci.2019.05.041.

[13] W. Wei et al., "Deep insights into the failure mechanisms in field-cycled ferroelectric $Hf_{0.5}Zr_{0.5}O_2$ thin film: TDDB characterizations and first-principles calculations," in *IEDM Tech. Dig.*, Dec. 2020, pp. 885–888, doi: 10.1109/IEDM13553.2020.9371932.

[14] K. Florent et al., "Investigation of the endurance of FE-HfO_2 devices by means of TDDB studies," in *Proc. IEEE Int. Rel. Phys. Symp. (IRPS)*, Mar. 2018, pp. 6D.3-1–6D.3-7, doi: 10.1109/IRPS.2018.8353634.

[15] P. D. Lomenzo et al., "TaN interface properties and electric field cycling effects on ferroelectric Si-doped HfO_2 thin films," *J. Appl. Phys.*, vol. 117, no. 13, Apr. 2015, Art. no. 134105, doi: 10.1063/1.4916715.

[16] E. D. Grimley et al., "Structural changes underlying field-cycling phenomena in ferroelectric HfO_2 thin films," *Adv. Electron. Mater.*, vol. 2, no. 9, Sep. 2016, Art. no. 1600173, doi: 10.1002/aelm.201600173.